Physics of Plasmas

RESEARCH ARTICLE | MAY 23 2025

Model-free Rayleigh weight from x-ray Thomson scattering measurements

T. Dornheim; H. M. Bellenbaum; M. Bethkenhagen; S. B. Hansen; M. P. Böhme; T. Döppner; L. B. Fletcher; T. Gawne; D. O. Gericke; S. Hamel; D. Kraus; M. J. MacDonald; Zh. A. Moldabekov; T. R. Preston; R. Redmer; M. Schörner; S. Schwalbe; P. Tolias; J. Vorberger

Phys. Plasmas 32, 052712 (2025)
https://doi.org/10.1063/5.0238630

Physics of Plasmas ARTICLE pubs.aip.org/aip/pop

Model-free Rayleigh weight from x-ray Thomson scattering measurements

Cite as: Phys. Plasmas **32**, 052712 (2025); doi: 10.1063/5.0238630
Submitted: 15 September 2024 · Accepted: 9 May 2025 ·
Published Online: 23 May 2025

T. Dornheim,[1,2,a)] H. M. Bellenbaum,[1] M. Bethkenhagen,[3] S. B. Hansen,[4] M. P. Böhme,[1,2,5] T. Döppner,[5] L. B. Fletcher,[6] T. Gawne,[1,2] D. O. Gericke,[7] S. Hamel,[5] D. Kraus,[2,8] M. J. MacDonald,[5] Zh. A. Moldabekov,[1,2] T. R. Preston,[9] R. Redmer,[8] M. Schörner,[8] S. Schwalbe,[1,2] P. Tolias,[10] and J. Vorberger[2]

AFFILIATIONS

[1]Center for Advanced Systems Understanding (CASUS), 02826 Görlitz, Germany
[2]Helmholtz-Zentrum Dresden-Rossendorf (HZDR), 01328 Dresden, Germany
[3]LULI, CNRS, CEA, Sorbonne Université, École Polytechnique – Institut Polytechnique de Paris, 91128 Palaiseau, France
[4]Sandia National Laboratories, Albuquerque, New Mexico 87185, USA
[5]Lawrence Livermore National Laboratory (LLNL), Livermore, California 94550, USA
[6]SLAC National Accelerator Laboratory, Menlo Park, California 94309, USA
[7]Centre for Fusion, Space and Astrophysics, Department of Physics, University of Warwick, Coventry CV4 7AL, United Kingdom
[8]Institut für Physik, Universität Rostock, 18051 Rostock, Germany
[9]European XFEL, 22869 Schenefeld, Germany
[10]Space and Plasma Physics, Royal Institute of Technology (KTH), Stockholm SE-100 44, Sweden

[a)]**Author to whom correspondence should be addressed:** t.dornheim@hzdr.de

ABSTRACT

X-ray Thomson scattering (XRTS) has emerged as a powerful tool for the diagnostics of matter under extreme conditions. In principle, it gives one access to important system parameters such as the temperature, density, and ionization state, but the interpretation of the measured XRTS intensity usually relies on theoretical models and approximations. In this context, a key property is given by the Rayleigh weight that describes the electronic localization around the ions. Here, we show that it is possible to extract the Rayleigh weight directly from the experimental data without the need for any model calculations or simulations. As a practical application, we consider an experimental measurement of strongly compressed Be at the National Ignition Facility [Döppner *et al.*, Nature **618**, 270–275 (2023)]. We demonstrate that experimental results for the Rayleigh weight open up new avenues for the interpretation of XRTS experiments by matching the measurement with *ab initio* simulations such as density functional theory or path integral Monte Carlo. Interestingly, this new procedure leads to significantly lower density compared to previously used chemical models.

INTRODUCTION

The x-ray Thomson scattering (XRTS) method[1,2] constitutes a powerful experimental technique, which is capable of giving microscopic insights into a probed sample. A particularly important use case for XRTS is the diagnostics of experiments with matter under extreme densities, temperatures, and pressures.[3] Such *warm dense matter* (WDM)[4,5] naturally occurs in various astrophysical objects such as giant planet interiors,[6–8] brown dwarfs,[9] and the outer crust of neutron stars.[10] Moreover, WDM plays an important role in a variety of technological applications such as inertial confinement fusion (ICF),[11] where the fuel capsule has to traverse the WDM regime in a controlled way to reach ignition ($\rho = 500$ g/cc, $T = 5 \times 10^7$ K).[12] The recent breakthrough at the National Ignition Facility (NIF) to reach ignition[13] has further substantiated the importance of accurately diagnosing WDM states. In the laboratory, these extreme states can be created in the laboratory using a variety of experimental techniques,[3] and XRTS is often used to infer *a priori* unknown system parameters such as the mass density ρ, temperature T, and ionization state Z; see, e.g., Ref. 14.

These properties can then be used for physical considerations, to inform equation-of-state tables[15–17] and to benchmark integrated multi-scale simulations such as radiation hydrodynamics.[18]

In practice, the measured XRTS intensity can be accurately expressed as[19]

$$I(\mathbf{q}, E) = S_{ee}(\mathbf{q}, E) \circledast R(E), \tag{1}$$

where $S_{ee}(\mathbf{q}, E)$ denotes the electronic dynamic structure factor (DSF) that describes the probed system, and $R(E)$ the combined source-and-instrument function (SIF) that takes into account the shape of the x-ray source and effects of the detector.[19] We note that a deconvolution solving Eq. (1) for $S_{ee}(\mathbf{q}, E)$ constitutes a major challenge considering the uncertainties of the SIF and the experimental error bars.[20,21] Therefore, the usual way to interpret the measured XRTS intensity has been to construct a forward model for $S_{ee}(\mathbf{q}, E)$, convolve it with $R(E)$, and then fit the resulting trial intensity to the LHS of Eq. (1) where the unknown system properties are treated as free parameters. Naturally, the thus inferred information depends on the employed forward model for $S_{ee}(\mathbf{q}, E)$. Although advances with *ab initio* methods have been made,[22] these models are usually based on a number of assumptions, such as the possibility to distinguish between *bound* and *free* electrons as proposed within the popular Chihara approach.[1,20,21,23–34]

Very recently, it has been proposed to instead consider the two-sided Laplace transform of the DSF,[5,37,38]

$$F_{ee}(\mathbf{q}, \tau) = \mathcal{L}[S_{ee}(\mathbf{q}, E)] = \int_{-\infty}^{\infty} \mathrm{d}E\, S_{ee}(\mathbf{q}, E)\, e^{-\tau E}, \tag{2}$$

which is directly related to the imaginary-time density–density correlation function (ITCF) $F_{ee}(\mathbf{q}, \tau)$. The latter naturally emerges in Feynman's path integral picture of statistical mechanics[39] and, from a physical perspective, contains the same information as $S_{ee}(\mathbf{q}, E)$, although in an unfamiliar representation.[40,41] It corresponds to the usual intermediate scattering function $F(\mathbf{q}, t) = \langle \hat{n}(\mathbf{q}, t)\hat{n}(-\mathbf{q}, 0)\rangle$ with an imaginary-time argument $t = -i\hbar\tau$ with $\tau \in [0, \beta]$ and $\beta = 1/k_{\mathrm{B}}T$ the inverse temperature. A key advantage of working in the Laplace domain is given by the convolution theorem

$$\mathcal{L}[S_{ee}(\mathbf{q}, E)] = \frac{\mathcal{L}[S_{ee}(\mathbf{q}, E) \circledast R(E)]}{\mathcal{L}[R(E)]}, \tag{3}$$

which is remarkably stable with respect to experimental noise.[35,38] Equation (3) thus gives one direct access to $F_{ee}(\mathbf{q}, \tau)$ from the experimental observation. As a first application, Dornheim *et al.*[37] have suggested to consider the imaginary-time version of the detailed balance relation $F_{ee}(\mathbf{q}, \tau) = F_{ee}(\mathbf{q}, \beta - \tau)$, which gives one model-free access to the temperature of arbitrarily complex systems.[34,37,38,42] A second practical application of the ITCF in the context of XRTS diagnostics is given by the f-sum rule, which relates the first τ-derivative of $F_{ee}(\mathbf{q}, \tau)$ to the momentum transfer $q = |\mathbf{q}|$ that follows from the scattering angle θ,[35,43] see Eq. (7), with m_e the electron mass. In this way, one can infer the normalization of the measured intensity, which is given by the electronic static structure factor $S_{ee}(\mathbf{q})$—the Fourier transform of the electron–electron pair correlation function $g_{ee}(\mathbf{r})$. Finally, we mention the recent idea by Vorberger *et al.*,[44] who have proposed to utilize Eq. (3) to quantify the degree of electronic non-equilibrium in the probed system.

In the present work, we extend these efforts toward a model-free diagnostics of XRTS measurements by extracting the Rayleigh weight $W_R(\mathbf{q}) = S_{eI}^2(\mathbf{q})/S_{II}(\mathbf{q})$ [where $S_{eI}(\mathbf{q})$ and $S_{II}(\mathbf{q})$ are the electron–ion and ion–ion static structure factor], which describes the degree of electronic localization around the ions,[45,46] directly from the experimental observation. Our idea is based on a combination of the f-sum rule with the ratio of elastic to inelastic scattering $r(\mathbf{q})$, cf. Eq. (5). Therefore, it is generally available and even extends to non-equilibrium situations. As a practical example, we consider an XRTS measurement on strongly compressed Be that has been carried out at the NIF;[33] see also Refs. 24, 25, 47, and 48 for previous experiments with warm dense Be. The proposed direct inference of $W_R(\mathbf{q})$ helps to further constrain forward models for the interpretation of XRTS measurements, which is very important in its own right. In addition, we expect $W_R(\mathbf{q})$ to be a valuable diagnostic tool. For example, one might first infer the temperature T from a given XRTS signal using the model-free ITCF method[37] and then carry out a set of *ab initio* calculations for $W_R(\mathbf{q})$ over a reasonable interval of densities ρ; here, we use highly accurate path integral Monte Carlo (PIMC) simulations using the setup described in Ref. 36 and density functional theory molecular dynamics (DFT-MD) simulations by Bethkenhagen *et al.*[49] We find excellent agreement between both methods in $W_R(\mathbf{q})$, whereas computationally less intensive average-atom models[30,50] and parameterized Chihara fits[1,28] deviate. This is of direct practical consequence for the interpretation of the experimental signal and suggests a significantly lower density of $\rho = (22 \pm 2)$ g/cc (see also Ref. 36) compared to the Chihara based estimate of $\rho = (34 \pm 4)$ g/cc by Döppner *et al.*[33]

From a methodological perspective, we note that $W_R(\mathbf{q})$ constitutes a perfect observable for DFT-MD, as it only involves the static single-electron density distribution $n_e(\mathbf{r})$ (and the ion density distribution and correlation function, which are both easily accessible within MD). This is in contrast to time-dependent DFT (TD-DFT) calculations that, in practice, contain additional approximations such as the unknown dynamic exchange–correlation kernel in the case of linear-response TD-DFT.[22,42,51,52] Finally, we mention the possibility to use experimental results for $W_R(\mathbf{q})$ as a rigorous benchmark for simulations and theoretical models in situations where the density and temperature are already known by other means.

IDEA

In general, when we can distinguish an elastic peak in an XRTS signal, we can split the DSF into a quasi-elastic contribution $S_{\mathrm{el}}(\mathbf{q}, E)$ described by the Rayleigh weight, and an inelastic part $S_{\mathrm{inel}}(\mathbf{q}, E)$ [cf. Fig. 1(a)],

$$S_{ee}(\mathbf{q}, E) = \underbrace{W_R(\mathbf{q})\delta(E)}_{S_{\mathrm{el}}(\mathbf{q},E)} + S_{\mathrm{inel}}(\mathbf{q}, E). \tag{4}$$

Here, the quasi-elastic nature of the first part is due to the substantially longer ionic timescales and localization of bound and nearly bound electrons around the ions. In practice, treating $S_{\mathrm{el}}(\mathbf{q}, E)$ as a delta distribution is appropriate if the SIF $R(E)$ is significantly broader than the actual ion feature. This is usually the case except for dedicated experiments that aim to resolve ionic energy scales.[53,54] Within the chemical picture that assumes a decomposition into effectively *bound* and *free* electrons,[1,28,32,33] the inelastic part $S_{\mathrm{inel}}(\mathbf{q}, E)$ consists of both transitions between bound and free states (and their reverse process[34]) and transitions between two free electronic states. The Rayleigh peak, too,

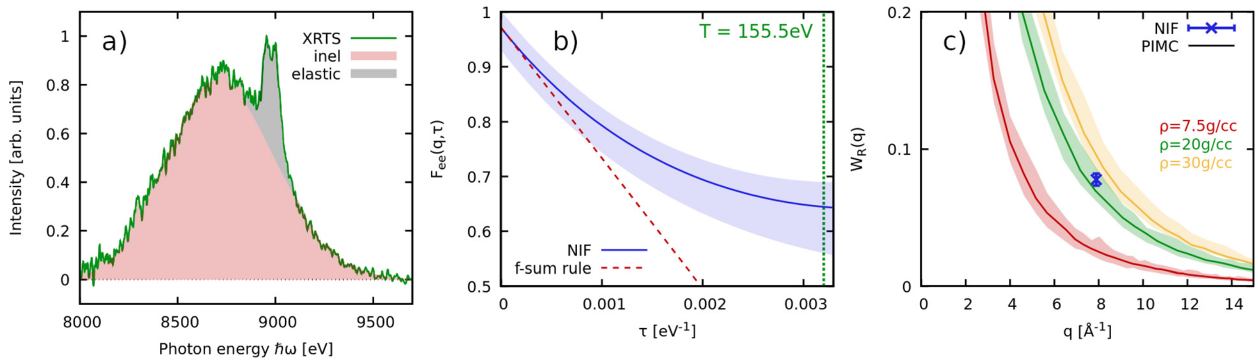

FIG. 1. (a) XRTS measurement on strongly compressed Be at the NIF[33] (green) and its decomposition into elastic (grey) and inelastic (red) contributions. (b) Determination of the normalization $S_{ee}(\mathbf{q}) = F_{ee}(\mathbf{q}, 0)$ from the f-sum rule,[35] cf. Eq. (7). (c) Wavenumber dependence of the Rayleigh weight $W_R(\mathbf{q})$, comparing the experimental data point [Eq. (6)] with *ab initio* PIMC simulations;[36] the solid lines have been obtained for $T = 155.5$ eV and the shaded areas correspond to the uncertainty range of ± 15 eV.

is informed by both free electrons (screening cloud) and bound electrons (form factor), and constitutes an indispensable ingredient to Chihara models[23,28,30] that are widely used for the interpretation of XRTS experiments with WDM.[1,32–34] However, it is important to note that we do not have to make such an approximate distinction between bound and free electrons in the present work as the computation of $W_R(q)$ only involves correlation functions between all electrons and ions, i.e., $S_{eI}(q)$ and $S_{II}(q)$.

Let us next consider the ratio of the elastic and inelastic contributions,

$$r(\mathbf{q}) = \frac{\int_{-\infty}^{\infty} d\omega\, S_{\text{el}}(\mathbf{q},\omega)}{\int_{-\infty}^{\infty} d\omega\, S_{\text{inel}}(\mathbf{q},\omega)} = \frac{W_R(\mathbf{q})}{S_{ee}(\mathbf{q}) - W_R(\mathbf{q})}, \tag{5}$$

that constitutes a standard observable in XRTS experiments,[33] see, e.g., Fig. 1(a). Here, $S_{ee}(\mathbf{q}) = F_{ee}(\mathbf{q}, 0)$ denotes the aforementioned electronic static structure factor that we can also directly extract from the XRTS signal using the f-sum rule applied in the imaginary-time domain as has been explained in detail in the recent Ref. 35, see also Eq. (7). Solving Eq. (5) for the Rayleigh weight then gives

$$W_R(\mathbf{q}) = \frac{S_{ee}(\mathbf{q})}{1 + r^{-1}(\mathbf{q})}. \tag{6}$$

RESULTS

In Fig. 1, we apply our new idea to an XRTS dataset that has been recently obtained at the NIF by Döppner *et al.*[33] Panel (a) shows the full XRTS intensity [solid green, cf. Eq. (1)], which can easily be decomposed into its elastic (gray) and inelastic (red) contribution if the SIF $R(E)$ is known; this is indeed the case for the backlighter x-ray source utilized at the NIF.[55] Note that we use the value of $r(\mathbf{q}) = 0.087 \pm 0.004$ from the original Ref. 33, which is consistent with an ionization of $Z = 3.4 \pm 0.1$. The second ingredient to Eq. (6) is given by the electronic static structure factor $S_{ee}(\mathbf{q})$, which we obtain from the Laplace transform of the XRTS signal via the f-sum rule. This procedure is illustrated in Fig. 1(b), where we show the deconvolved $F_{ee}(\mathbf{q}, \tau)$ as a function of τ. In the imaginary-time domain, the f-sum rule is given by[35,40,43]

$$\frac{\partial}{\partial \tau} F_{ee}(\mathbf{q}, \tau)\Big|_{\tau=0} = -\frac{\hbar^2 \mathbf{q}^2}{2m_e}; \tag{7}$$

matching Eq. (7) (dashed red line) with the LHS of Eq. (3) (solid blue line) around $\tau = 0$ then determines the *a priori* unknown normalization constant and, in turn, $S_{ee}(\mathbf{q}) = F_{ee}(\mathbf{q}, 0)$. Inserting $r(\mathbf{q})$ and $S_{ee}(\mathbf{q})$ into Eq. (6) gives our final, model-free estimate of the Rayleigh weight, which is shown as the blue cross in Fig. 1(c) at the corresponding experimental wavenumber of $q = 7.89$ Å^{-1}. The red, green, and yellow solid curves in the panel show *ab initio* PIMC results that have been obtained for $N_{\text{Be}} = 10$ Be atoms using the setup described in recent studies,[36,56] at the temperature of $T = 155.5$ eV that has been inferred from the symmetry of the ITCF; see the appendix of Ref. 36 for additional details. In addition, the associated colored areas correspond to PIMC simulations for $T = (155.5 \pm 15)$ eV and indicate the uncertainty in the Rayleigh weight at a given density due to the uncertainty in the inferred temperature. Figure 1 thus indicates a mass density of $\rho \approx 20$ g/cc, whereas the nominal result of $\rho = (34 \pm 4)$ g/cc reported in the original Ref. 33 is ruled out.

For further insight into the sensitivity of the interpretation of a given XRTS measurement to the employed model or simulation technique, we compare a number of independent methods in Fig. 2, where the top and bottom panels correspond to $\rho = 20$ g/cc and $\rho = 30$ g/cc, respectively. For both cases, we find very good agreement between PIMC (solid green) and DFT-MD simulations by Bethkenhagen *et al.*[49] (dash-dotted purple). The computationally cheaper average-atom model[30,50] (dashed red) is in qualitative, though not quantitative agreement with the *ab initio* datasets. Instead, it agrees with the experimental data point for $\rho = 30$ g/cc. This highlights the sensitivity of equation-of-state measurements to the proper treatment of electronic correlations and other many-body effects in the analysis of the experimental observation. At the same time, we note the comparably high computation effort of PIMC and DFT-MD ($\sim \mathcal{O}(10^5)$ CPUh per calculation) compared to AA ($\sim \mathcal{O}(10^{-1})$ CPUh per calculation). Finally, we include two chemical models for the hypothetical ionization degrees of $Z = 3.52$ (dotted black) and $Z = 3.73$ (dotted yellow) for both densities, see the supplementary material for additional details. Evidently, the inferred density strongly depends on the inferred ionization state, making the invocation of additional constraints desirable. In Ref. 33, Döppner *et al.* have used the Saha

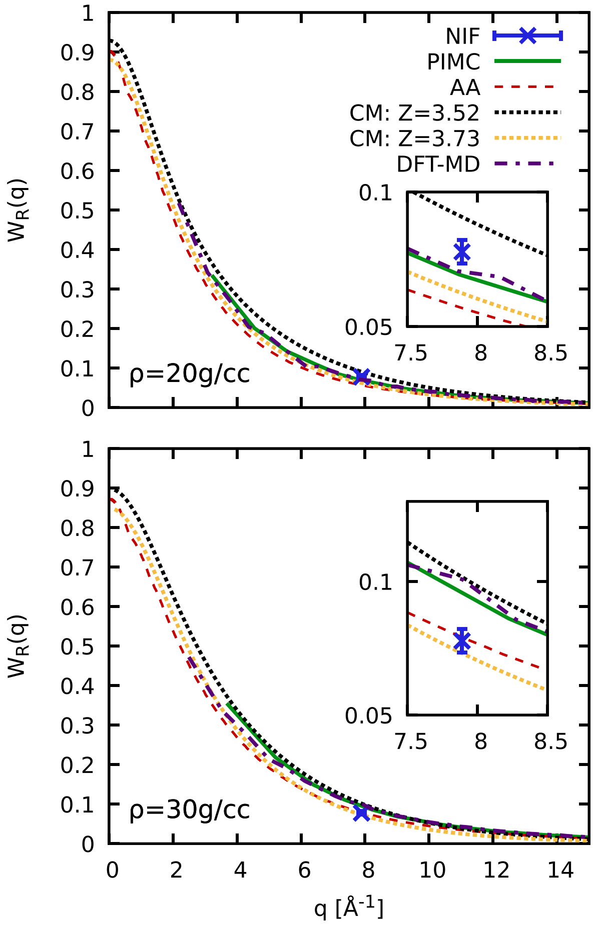

FIG. 2. Comparison of simulation results for the Rayleigh weight at $\rho = 20$ g/cc (top) and $\rho = 30$ g/cc (bottom). Blue cross: experiment;[33] solid green: PIMC; dashed red: average atom model; black and yellow dotted: chemical model with ionization states of $Z = 3.52$ and $Z = 3.73$; and dash-dotted purple: DFT-MD.[49] PIMC and CM have been computed for $T = 155.5$ eV, DFT-MD and AA for $T = 150$ eV.

equation in combination with a semi-empirical form factor lowering model for this purpose, leading to the nominal parameters of $\rho = (34 \pm 4)$ g/cc and $Z = 3.4 \pm 0.1$. A systematic investigation of the origin of this discrepancy between their chemical model and the *ab initio* datasets from PIMC and DFT-MD is beyond the scope of the present work and will be pursued in a dedicated future study.

Let us conclude with a systematic analysis of the dependence of $W_R(\mathbf{q})$ on the density, as shown in Fig. 3 based on extensive DFT-MD results for $\rho = (5-80)$ g/cc at $T = 150$ eV. The main trend is given by the systematic increase in the Rayleigh weight with ρ, which is to a large degree due to the different length scales in the system; the effect almost vanishes when one adjusts the x axis by the Fermi wavenumber $q_F \sim 1/\rho^{1/3}$. The inset shows a magnified segment around the experimental data point, with the latter being located between the DFT-MD results for $\rho = 20$ g/cc (red) and $\rho = 24$ g/cc (black); this leads to our final estimate for the density of $\rho = (22 \pm 2)$ g/cc (dash-dotted pink).

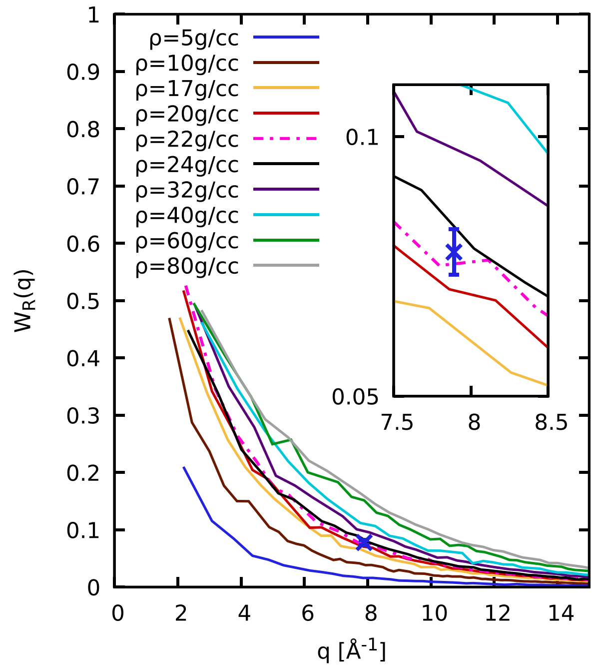

FIG. 3. Curves: DFT-MD results for $W_R(\mathbf{q})$ at $T = 150$ eV for different mass densities ρ. The experimental measurement (blue cross) at the NIF[33] is associated with a density of $\rho = 22 \pm 2$ g/cc (dash-dotted pink), see also the inset showing a magnified segment.

SUMMARY AND DISCUSSION

We have presented a new approach for the model-free extraction of the Rayleigh weight $W_R(\mathbf{q})$ from XRTS measurements. Most importantly, $W_R(\mathbf{q})$ constitutes an important measure for the electronic localization around the ions, which is related to multiple possible definitions of the average ion charge[57] and interesting in its own right. In addition, $W_R(\mathbf{q})$ is of direct practical value for XRTS diagnostics, as we have demonstrated in detail in a recent experiment with strongly compressed beryllium at the NIF.[33] In particular, we propose to first infer the temperature T from the model-free ITCF thermometry approach[37,38] and to subsequently match the experimental result for $W_R(\mathbf{q})$ with simulation results over a reasonable range of densities. We note that $W_R(\mathbf{q})$ is a particularly suitable observable for DFT-MD simulations, as it does not involve any dynamic information such as the *a priori* unknown dynamic exchange–correlation kernel. We find excellent agreement between DFT-MD and PIMC reference data; this is encouraging since direct PIMC simulations are still limited to low-Z materials at moderate to high temperatures,[58,59] whereas DFT-MD and TD-DFT[22,60] are more broadly applicable. An additional advantage of $W_R(\mathbf{q})$ over alternative observables such as the ratio of elastic to inelastic scattering $r(\mathbf{q})$ is that the former does not require any explicit information about the electronic static structure factor $S_{ee}(\mathbf{q})$, which is notoriously difficult for DFT-based methodologies.

In practice, we infer a mass density of $\rho = (22 \pm 2)$ g/cc from the beryllium dataset using either PIMC or DFT-MD simulations, which is significantly lower than the nominal value of $\rho = (34 \pm 4)$ g/cc that has been reported in the original publication based on a chemical Chihara model; note that the latter must take into account a proper multi-component treatment of differently charged ions.[61] Moreover, we find that the computationally more efficient average-atom model tends to overestimate the density, whereas chemical models generally require additional constraints for parameters such as the ionization degree. Our study thus clearly highlights the importance of an accurate treatment of quantum many-body effects for XRTS based equation-of-state measurements even at relatively high temperatures.

This work opens up new possibilities for the study of warm dense matter and beyond. An important point for future research is given by the sensitivity of the inferred Rayleigh weight to the SIF $R(E)$, which is usually modeled for backlighter setups[55] but can be known with high precision at modern XFEL facilities.[19] Indeed, recent advances in high-resolution XRTS measurements[60] at the European XFEL will likely facilitate the application of the model-free ITCF thermometry technique even at moderate temperatures of $T \sim 1$ eV, which are of relevance for both planetary and materials science; the current model-free framework for the extraction of $W_R(\mathbf{q})$ is applicable at any temperature. In combination, these two methods will allow for accurate equation-of-state measurements in previously inaccessible regimes. Finally, we mention the intriguing possibility of performing an XRTS experiment on an isochorically heated sample with an appropriate delay between pump and probe to ensure proper equilibration. Since both T and ρ would be well known in such a scenario, a corresponding measurement of $W_R(\mathbf{q})$ using the present framework would constitute a truly unambiguous reference dataset for the rigorous benchmarking of *ab initio* simulations and chemical models alike.

SUPPLEMENTARY MATERIAL

See the supplementary material for additional information about the extraction of the experimental data point for the Rayleigh weight, as well as a discussion of the range of applicability and limitations of the method. In addition, we provide details on the presented PIMC, DFT-MD, average atom, and chemical model calculations.

ACKNOWLEDGMENTS

This work was partially supported by the Center for Advanced Systems Understanding (CASUS), financed by Germany's Federal Ministry of Education and Research (BMBF) and the Saxon state government out of the State budget approved by the Saxon State Parliament. This work has received funding from the European Union's Just Transition Fund (JTF) within the project *Röntgenlaser-Optimierung der Laserfusion* (ROLF), Contract No. 5086999001, co-financed by the Saxon state government out of the State budget approved by the Saxon State Parliament. This work has received funding from the European Research Council (ERC) under the European Union's Horizon 2022 research and innovation programme (Grant agreement No. 101076233, "PREXTREME"). The work of Ti.D., M.P.B, S.H., and M.J.M. was performed under the auspices of the U.S. Department of Energy by Lawrence Livermore National Laboratory under Contract No. DE-AC52-07NA27344. Ti.D., M.P.B., M.J.M., and D.O.G. were supported by Laboratory Directed Research and Development (LDRD) Grant Nos. 24-ERD-044 and 25-ERD-047. This work was partially supported by the German Research Foundation (DFG) within the Research Unit FOR 2440. Views and opinions expressed are, however, those of the authors only and do not necessarily reflect those of the European Union or the European Research Council Executive Agency. Neither the European Union nor the granting authority can be held responsible for them. Computations were performed on a Bull Cluster at the Center for Information Services and High-Performance Computing (ZIH) at Technische Universität Dresden and at the Norddeutscher Verbund für Hoch- und Höchstleistungsrechnen (HLRN) under Grant Nos. mvp00018 and mvp00024. S.B.H. was supported by Sandia National Laboratories, a multi-mission laboratory managed and operated by National Technology and Engineering Solutions of Sandia, LLC, a wholly owned subsidiary of Honeywell International, Inc., for DOE's National Nuclear Security Administration under contract DE-NA0003525. This paper describes objective technical results and analysis. Any subjective views or opinions that might be expressed in the paper do not necessarily represent the views of the U.S. Department of Energy or the United States Government. The work of LBF is supported by the DOE Office of Science, Fusion Energy Science under FWP 100866, and supported by the Department of Energy, Laboratory Directed Research and Development program at SLAC National Accelerator Laboratory, under Contract No. DE-AC02-76SF00515.

AUTHOR DECLARATIONS

Conflict of Interest

The authors have no conflicts to disclose.

Author Contributions

T. Dornheim: Conceptualization (equal); Investigation (lead); Project administration (equal); Writing – original draft (equal). **H. M. Bellenbaum:** Investigation (equal); Project administration (equal); Writing – original draft (equal). **M. Bethkenhagen:** Investigation (equal); Writing – review & editing (equal). **S. B. Hansen:** Investigation (equal); Writing – review & editing (equal). **M. P. Böhme:** Investigation (equal); Writing – review & editing (equal). **T. Döppner:** Investigation (equal); Writing – review & editing (equal). **L. B. Fletcher:** Investigation (equal); Writing – review & editing (equal). **T. Gawne:** Investigation (equal); Writing – review & editing (equal). **D. O. Gericke:** Investigation (equal); Writing – review & editing (equal). **S. Hamel:** Investigation (equal); Writing – review & editing (equal). **D. Kraus:** Investigation (equal); Writing – review & editing (equal). **M. J. MacDonald:** Investigation (equal); Writing – review & editing (equal). **Zh. A. Moldabekov:** Investigation (equal); Writing – review & editing (equal). **T. R. Preston:** Investigation (equal); Writing – review & editing (equal). **R. Redmer:** Investigation (equal); Writing – review & editing (equal). **M. Schörner:** Investigation (equal); Writing – review & editing (equal). **S. Schwalbe:** Investigation (equal); Writing – review & editing (equal). **P. Tolias:** Investigation (equal); Writing – review & editing (equal). **J. Vorberger:** Investigation (equal); Writing – review & editing (equal).

DATA AVAILABILITY

The data that support the findings of this study are available from the corresponding author upon reasonable request.

REFERENCES

[1] S. H. Glenzer and R. Redmer, "X-ray Thomson scattering in high energy density plasmas," Rev. Mod. Phys. **81**, 1625 (2009).
[2] J. Sheffield, D. Froula, S. H. Glenzer, and N. C. Luhmann, *Plasma Scattering of Electromagnetic Radiation: Theory and Measurement Techniques* (Elsevier Science, 2010).

[3]K. Falk, "Experimental methods for warm dense matter research," High Power Laser Sci. Eng. **6**, e59 (2018).
[4]*Frontiers and Challenges in Warm Dense Matter*, edited by F. Graziani, M. P. Desjarlais, R. Redmer, and S. B. Trickey (Springer International Publishing, 2014).
[5]T. Dornheim, Z. A. Moldabekov, K. Ramakrishna, P. Tolias, A. D. Baczewski, D. Kraus, Th. R. Preston, D. A. Chapman, M. P. Böhme, T. Döppner, F. Graziani, M. Bonitz, A. Cangi, and J. Vorberger, "Electronic density response of warm dense matter," Phys. Plasmas **30**, 032705 (2023).
[6]A. Benuzzi-Mounaix, S. Mazevet, A. Ravasio, T. Vinci, A. Denoeud, M. Koenig, N. Amadou, E. Brambrink, F. Festa, A. Levy, M. Harmand, S. Brygoo, G. Huser, V. Recoules, J. Bouchet, G. Morard, F. Guyot, T. de Resseguier, K. Myanishi, N. Ozaki, F. Dorchies, J. Gaudin, P. M. Leguay, O. Peyrusse, O. Henry, D. Raffestin, S. L. Pape, R. Smith, and R. Musella, "Progress in warm dense matter study with applications to planetology," Phys. Scr. **2014**(T161), 014060.
[7]T. Guillot, L. N. Fletcher, R. Helled, M. Ikoma, M. R. Line, and V. Parmentier, "Giant planets from the inside-out," arXiv:2205.04100 (2022).
[8]R. P. Drake, *High-Energy-Density Physics: Foundation of Inertial Fusion and Experimental Astrophysics, Graduate Texts in Physics* (Springer International Publishing, 2018).
[9]A. Becker, W. Lorenzen, J. J. Fortney, N. Nettelmann, M. Schöttler, and R. Redmer, "Ab initio equations of state for hydrogen (H-REOS.3) and helium (He-REOS.3) and their implications for the interior of brown dwarfs," Astrophys. J. Suppl. Ser. **215**, 21 (2014).
[10]E. H. Gudmundsson, C. J. Pethick, and R. I. Epstein, "Structure of neutron star envelopes," Astrophys. J. **272**, 286–300 (1983).
[11]R. Betti and O. A. Hurricane, "Inertial-confinement fusion with lasers," Nat. Phys. **12**, 435–448 (2016).
[12]S. X. Hu, B. Militzer, V. N. Goncharov, and S. Skupsky, "First-principles equation-of-state table of deuterium for inertial confinement fusion applications," Phys. Rev. B **84**, 224109 (2011).
[13]: H. Abu-Shawareb, R. Acree, P. Adams, J. Adams, B. Addis, R. Aden, P. Adrian, B. B. Afeyan, M. Aggleton, L. Aghaian, The Indirect Drive ICF Collaboration *et al.*, "Achievement of target gain larger than unity in an inertial fusion experiment," Phys. Rev. Lett. **132**, 065102 (2024).
[14]K.-U. Plagemann, H. R. Rüter, T. Bornath, M. Shihab, M. P. Desjarlais, C. Fortmann, S. H. Glenzer, and R. Redmer, "*Ab initio* calculation of the ion feature in x-ray Thomson scattering," Phys. Rev. E **92**, 013103 (2015).
[15]K. Falk, S. P. Regan, J. Vorberger, M. A. Barrios, T. R. Boehly, D. E. Fratanduono, S. H. Glenzer, D. G. Hicks, S. X. Hu, C. D. Murphy, P. B. Radha, S. Rothman, A. P. Jephcoat, J. S. Wark, D. O. Gericke, and G. Gregori, "Self-consistent measurement of the equation of state of liquid deuterium," High Energy Density Phys. **8**, 76–80 (2012).
[16]K. Falk, E. J. Gamboa, G. Kagan, D. S. Montgomery, B. Srinivasan, P. Tzeferacos, and J. F. Benage, "Equation of state measurements of warm dense carbon using laser-driven shock and release technique," Phys. Rev. Lett. **112**, 155003 (2014).
[17]J. A. Gaffney, S. X. Hu, P. Arnault, A. Becker, L. X. Benedict, T. R. Boehly, P. M. Celliers, D. M. Ceperley, O. Čertík, J. Clérouin, G. W. Collins, L. A. Collins, J.-F. Danel, N. Desbiens, M. W. C. Dharma-Wardana, Y. H. Ding, A. Fernandez-Pañella, M. C. Gregor, P. E. Grabowski, S. Hamel, S. B. Hansen, L. Harbour, X. T. He, D. D. Johnson, W. Kang, V. V. Karasiev, L. Kazandjian, M. D. Knudson, T. Ogitsu, C. Pierleoni, R. Piron, R. Redmer, G. Robert, D. Saumon, A. Shamp, T. Sjostrom, A. V. Smirnov, C. E. Starrett, P. A. Sterne, A. Wardlow, H. D. Whitley, B. Wilson, P. Zhang, and E. Zurek, "A review of equation-of-state models for inertial confinement fusion materials," High Energy Density Phys. **28**, 7–24 (2018).
[18]G. C. Pomraning, *The Equations of Radiation Hydrodynamics, Dover Books on Physics* (Dover Publications, 2005).
[19]T. Gawne, H. M. Bellenbaum, L. B. Fletcher, K. Appel, C. Baehtz, V. Bouffetier, E. Brambrink, D. Brown, A. Cangi, A. Descamps, S. Goede, N. J. Hartley, M.-L. Herbert, P. Hesselbach, H. Höppner, O. S. Humphries, Z. Konôpková, A. Laso Garcia, B. Lindqvist, J. Lütgert, M. J. MacDonald, M. Makita, W. Martin, M. Mishchenko, Z. A. Moldabekov, M. Nakatsutsumi, J.-P. Naedler, P. Neumayer, A. Pelka, C. Qu, L. Randolph, J. Rips, T. Toncian, J. Vorberger, L. Wollenweber, U. Zastrau, D. Kraus, T. R. Preston, and T. Dornheim, "Effects of mosaic crystal instrument functions on x-ray Thomson scattering diagnostics," J. Appl. Phys. **136**, 105902 (2024).
[20]A. Höll, T. Bornath, L. Cao, T. Döppner, S. Düsterer, E. Förster, C. Fortmann, S. H. Glenzer, G. Gregori, T. Laarmann, K.-H. Meiwes-Broer, A. Przystawik, P. Radcliffe, R. Redmer, H. Reinholz, G. Röpke, R. Thiele, J. Tiggesbäumker, S. Toleikis, N. X. Truong, T. Tschentscher, I. Uschmann, and U. Zastrau, "Thomson scattering from near-solid density plasmas using soft x-ray free electron lasers," High Energy Density Phys. **3**, 120–130 (2007).
[21]C. Fortmann, T. Bornath, R. Redmer, H. Reinholz, G. Röpke, V. Schwarz, and R. Thiele, "X-ray Thomson scattering cross-section in strongly correlated plasmas," Laser Part. Beams **27**, 311–319 (2009).
[22]A. D. Baczewski, L. Shulenburger, M. P. Desjarlais, S. B. Hansen, and R. J. Magyar, "X-ray Thomson scattering in warm dense matter without the Chihara decomposition," Phys. Rev. Lett. **116**, 115004 (2016).
[23]J. Chihara, "Difference in x-ray scattering between metallic and non-metallic liquids due to conduction electrons," J. Phys. F **17**, 295–304 (1987).
[24]S. H. Glenzer, O. L. Landen, P. Neumayer, R. W. Lee, K. Widmann, S. W. Pollaine, R. J. Wallace, G. Gregori, A. Höll, T. Bornath, R. Thiele, V. Schwarz, W.-D. Kraeft, and R. Redmer, "Observations of plasmons in warm dense matter," Phys. Rev. Lett. **98**, 065002 (2007).
[25]H. J. Lee, P. Neumayer, J. Castor, T. Döppner, R. W. Falcone, C. Fortmann, B. A. Hammel, A. L. Kritcher, O. L. Landen, R. W. Lee, D. D. Meyerhofer, D. H. Munro, R. Redmer, S. P. Regan, S. Weber, and S. H. Glenzer, "X-ray Thomson-scattering measurements of density and temperature in shock-compressed beryllium," Phys. Rev. Lett. **102**, 115001 (2009).
[26]H. J. Lee, T. Döppner, P. Neumayer, J. Castor, R. W. Falcone, C. Fortmann, B. A. Hammel, A. L. Kritcher, O. L. Landen, R. W. Lee, D. D. Meyerhofer, D. H. Munro, R. Redmer, S. P. Regan, S. Weber, R. Wallace, and S. H. Glenzer, "X-ray Thomson scattering measurement in shock-compressed beryllium," J. Phys. Conf. Ser. **244**, 042015 (2010).
[27]T. Döppner, C. Fortmann, P. F. Davis, A. L. Kritcher, O. L. Landen, H. J. Lee, R. Redmer, S. P. Regan, and S. H. Glenzer, "X-ray Thomson scattering for measuring dense beryllium plasma collisionality," J. Phys. Conf. Ser. **244**, 032044 (2010).
[28]G. Gregori, S. H. Glenzer, W. Rozmus, R. W. Lee, and O. L. Landen, "Theoretical model of x-ray scattering as a dense matter probe," Phys. Rev. E **67**, 026412 (2003).
[29]W. R. Johnson, J. Nilsen, and K. T. Cheng, "Thomson scattering in the average-atom approximation," Phys. Rev. E **86**, 036410 (2012).
[30]A. N. Souza, D. J. Perkins, C. E. Starrett, D. Saumon, and S. B. Hansen, "Predictions of x-ray scattering spectra for warm dense matter," Phys. Rev. E **89**, 023108 (2014).
[31]B. A. Mattern, G. T. Seidler, J. J. Kas, J. I. Pacold, and J. J. Rehr, "Real-space Green's function calculations of Compton profiles," Phys. Rev. B **85**, 115135 (2012).
[32]D. Kraus, B. Bachmann, B. Barbrel, R. W. Falcone, L. B. Fletcher, S. Frydrych, E. J. Gamboa, M. Gauthier, D. O. Gericke, S. H. Glenzer, S. Göde, E. Granados, N. J. Hartley, J. Helfrich, H. J. Lee, B. Nagler, A. Ravasio, W. Schumaker, J. Vorberger, and T. Döppner, "Characterizing the ionization potential depression in dense carbon plasmas with high-precision spectrally resolved x-ray scattering," Plasma Phys. Controlled Fusion **61**, 014015 (2019).
[33]T. Döppner, M. Bethkenhagen, D. Kraus, P. Neumayer, D. A. Chapman, B. Bachmann, R. A. Baggott, M. P. Böhme, L. Divol, R. W. Falcone, L. B. Fletcher, O. L. Landen, M. J. MacDonald, A. M. Saunders, M. Schörner, P. A. Sterne, J. Vorberger, B. B. L. Witte, A. Yi, R. Redmer, S. H. Glenzer, and D. O. Gericke, "Observing the onset of pressure-driven K-shell delocalization," Nature **618**, 270–275 (2023).
[34]M. P. Böhme, L. B. Fletcher, T. Döppner, D. Kraus, A. D. Baczewski, T. R. Preston, M. J. MacDonald, F. R. Graziani, Z. A. Moldabekov, J. Vorberger, and T. Dornheim, "Evidence of free-bound transitions in warm dense matter and their impact on equation-of-state measurements," arXiv:2306.17653 (2023).
[35]T. Dornheim, T. Döppner, A. D. Baczewski, P. Tolias, M. P. Böhme, Z. A. Moldabekov, T. Gawne, D. Ranjan, D. A. Chapman, M. J. MacDonald, T. R. Preston, D. Kraus, and J. Vorberger, "X-ray Thomson scattering absolute intensity from the f-sum rule in the imaginary-time domain," Sci. Rep. **14**, 14377 (2024).

[36]T. Dornheim, T. Döppner, P. Tolias, M. Böhme, L. Fletcher, T. Gawne, F. Graziani, D. Kraus, M. MacDonald, Z. Moldabekov, S. Schwalbe, D. Gericke, and J. Vorberger, "Unraveling electronic correlations in warm dense quantum plasmas," arXiv:2402.19113 (2024).
[37]T. Dornheim, M. Böhme, D. Kraus, T. Döppner, T. R. Preston, Z. A. Moldabekov, and J. Vorberger, "Accurate temperature diagnostics for matter under extreme conditions," Nat. Commun. **13**, 7911 (2022).
[38]T. Dornheim, M. P. Böhme, D. A. Chapman, D. Kraus, T. R. Preston, Z. A. Moldabekov, N. Schlünzen, A. Cangi, T. Döppner, and J. Vorberger, "Imaginary-time correlation function thermometry: A new, high-accuracy and model-free temperature analysis technique for x-ray Thomson scattering data," Phys. Plasmas **30**, 042707 (2023).
[39]H. Kleinert, *Path Integrals in Quantum Mechanics, Statistics, Polymer Physics, and Financial Markets*, EBL-Schweitzer (World Scientific, 2009).
[40]T. Dornheim, Z. Moldabekov, P. Tolias, M. Böhme, and J. Vorberger, "Physical insights from imaginary-time density–density correlation functions," Matter Radiat. Extremes **8**, 056601 (2023).
[41]T. Dornheim, J. Vorberger, Z. A. Moldabekov, and M. Böhme, "Analysing the dynamic structure of warm dense matter in the imaginary-time domain: Theoretical models and simulations," Philos. Trans. R. Soc. A **381**, 20220217 (2023).
[42]M. Schörner, M. Bethkenhagen, T. Döppner, D. Kraus, L. B. Fletcher, S. H. Glenzer, and R. Redmer, "X-ray Thomson scattering spectra from density functional theory molecular dynamics simulations based on a modified Chihara formula," Phys. Rev. E **107**, 065207 (2023).
[43]T. Dornheim, D. C. Wicaksono, J. E. Suarez-Cardona, P. Tolias, M. P. Böhme, Z. A. Moldabekov, M. Hecht, and J. Vorberger, "Extraction of the frequency moments of spectral densities from imaginary-time correlation function data," Phys. Rev. B **107**, 155148 (2023).
[44]J. Vorberger, T. R. Preston, N. Medvedev, M. P. Böhme, Z. A. Moldabekov, D. Kraus, and T. Dornheim, "Revealing non-equilibrium and relaxation in laser heated matter," Phys. Lett. A **499**, 129362 (2024).
[45]J. Vorberger and D. O. Gericke, "*Ab initio* approach to model x-ray diffraction in warm dense matter," Phys. Rev. E **91**, 033112 (2015).
[46]T. Ma, T. Döppner, R. W. Falcone, L. Fletcher, C. Fortmann, D. O. Gericke, O. L. Landen, H. J. Lee, A. Pak, J. Vorberger, K. Wünsch, and S. H. Glenzer, "X-ray scattering measurements of strong ion-ion correlations in shock-compressed aluminum," Phys. Rev. Lett. **110**, 065001 (2013).
[47]C. Fortmann, H. J. Lee, T. Döppner, R. W. Falcone, A. L. Kritcher, O. L. Landen, and S. H. Glenzer, "Measurement of the adiabatic index in be compressed by counterpropagating shocks," Phys. Rev. Lett. **108**, 175006 (2012).
[48]S. H. Glenzer, G. Gregori, F. J. Rogers, D. H. Froula, S. W. Pollaine, R. S. Wallace, and O. L. Landen, "X-ray scattering from solid density plasmas," Phys. Plasmas **10**, 2433–2441 (2003).
[49]M. Bethkenhagen, M. Schörner, and R. Redmer, "Insights on the electronic structure of high-density beryllium from ab initio simulations" (submitted).
[50]P. A. Sterne, S. B. Hansen, B. G. Wilson, and W. A. Isaacs, "Equation of state, occupation probabilities and conductivities in the average atom Purgatorio code," High Energy Density Phys. **3**, 278–282 (2007).
[51]Z. Moldabekov, M. Böhme, J. Vorberger, D. Blaschke, and T. Dornheim, "Ab Initio static exchange–correlation Kernel across Jacob's Ladder without functional derivatives," J. Chem. Theory Comput. **19**, 1286–1299 (2023).
[52]Z. A. Moldabekov, M. Pavanello, M. P. Böhme, J. Vorberger, and T. Dornheim, "Linear-response time-dependent density functional theory approach to warm dense matter with adiabatic exchange-correlation kernels," Phys. Rev. Res. **5**, 023089 (2023).
[53]A. Descamps, B. K. Ofori-Okai, K. Appel, V. Cerantola, A. Comley, J. H. Eggert, L. B. Fletcher, D. O. Gericke, S. Göde, O. Humphries, O. Karnbach, A. Lazicki, R. Loetzsch, D. McGonegle, C. A. J. Palmer, C. Plueckthun, T. R. Preston, R. Redmer, D. G. Senesky, C. Strohm, I. Uschmann, T. G. White, L. Wollenweber, G. Monaco, J. S. Wark, J. B. Hastings, U. Zastrau, G. Gregori, S. H. Glenzer, and E. E. McBride, "An approach for the measurement of the bulk temperature of single crystal diamond using an x-ray free electron laser," Sci. Rep. **10**, 14564 (2020).
[54]T. G. White, H. Poole, E. E. McBride, M. Oliver, A. Descamps, L. B. Fletcher, W. A. Angermeier, C. H. Allen, K. Appel, F. P. Condamine, C. B. Curry, F. Dallari, S. Funk, E. Galtier, E. J. Gamboa, M. Gauthier, P. Graham, S. Goede, D. Haden, J. B. Kim, H. J. Lee, B. K. Ofori-Okai, S. Richardson, A. Rigby, C. Schoenwaelder, P. Sun, B. L. Witte, T. Tschentscher, U. Zastrau, B. Nagler, J. B. Hastings, G. Monaco, D. O. Gericke, S. H. Glenzer, and G. Gregori, "Speed of sound in methane under conditions of planetary interiors," Phys. Rev. Res. **6**, L022029 (2024).
[55]M. J. MacDonald, A. M. Saunders, B. Bachmann, M. Bethkenhagen, L. Divol, M. D. Doyle, L. B. Fletcher, S. H. Glenzer, D. Kraus, O. L. Landen, H. J. LeFevre, S. R. Klein, P. Neumayer, R. Redmer, M. Schörner, N. Whiting, R. W. Falcone, and T. Döppner, "Demonstration of a laser-driven, narrow spectral bandwidth x-ray source for collective x-ray scattering experiments," Phys. Plasmas **28**, 032708 (2021).
[56]T. Dornheim, S. Schwalbe, M. Böhme, Z. Moldabekov, J. Vorberger, and P. Tolias, "*Ab initio* path integral Monte Carlo simulations of warm dense two-component systems without fixed nodes: Structural properties," J. Chem. Phys. **160**, 164111 (2024).
[57]M. S. Murillo, J. Weisheit, S. B. Hansen, and M. W. C. Dharma-Wardana, "Partial ionization in dense plasmas: Comparisons among average-atom density functional models," Phys. Rev. E **87**, 063113 (2013).
[58]T. Dornheim, "Fermion sign problem in path integral Monte Carlo simulations: Quantum dots, ultracold atoms, and warm dense matter," Phys. Rev. E **100**, 023307 (2019).
[59]M. Bonitz, J. Vorberger, M. Bethkenhagen, M. P. Böhme, D. M. Ceperley, A. Filinov, T. Gawne, F. Graziani, G. Gregori, P. Hamann, S. B. Hansen, M. Holzmann, S. X. Hu, H. Kählert, V. V. Karasiev, U. Kleinschmidt, L. Kordts, C. Makait, B. Militzer, Z. A. Moldabekov, C. Pierleoni, M. Preising, K. Ramakrishna, R. Redmer, S. Schwalbe, P. Svensson, and T. Dornheim, "Toward first principles-based simulations of dense hydrogen," Phys. Plasmas **31**, 110501 (2024).
[60]T. Gawne, Z. A. Moldabekov, O. S. Humphries, K. Appel, C. Baehtz, V. Bouffetier, E. Brambrink, A. Cangi, S. Göde, Z. Konôpková, M. Makita, M. Mishchenko, M. Nakatsutsumi, K. Ramakrishna, L. Randolph, S. Schwalbe, J. Vorberger, L. Wollenweber, U. Zastrau, T. Dornheim, and T. R. Preston, "Ultrahigh resolution x-ray Thomson scattering measurements at the European X-ray free electron laser," Phys. Rev. B **109**, L241112 (2024).
[61]K. Wünsch, J. Vorberger, G. Gregori, and D. O. Gericke, "X-ray scattering as a probe for warm dense mixtures and high-pressure miscibility," Europhys. Lett. **94**, 25001 (2011).